THERMO-HYDRAULIC ANALYSIS OF A SMALL MODULAR REACTOR OF TYPE IPWR

ANÁLISIS TERMO-HIDRÁULICO DE UN REACTOR MODULAR PEQUEÑO DE TIPO IPWR

D. Perdigón[a†], C. García[a], J. Rosales[b], L. Rojas[c], S. Almira[a]

a) Instituto Superior de Tecnologías y Ciencias Aplicadas, Universidad de la Habana, Cuba. perdigondc99@gmail.com†
b) Universidad Nacional Autónoma de México, México.
c) Universidade Federal de Pernambuco, Brasil.
† corresponding author

Recibido 05/12/2023; Aceptado 01/05/2024

Small Modular Reactors (SMRs) are an innovative option for power generation. This type of reactor offers numerous benefits and uses. The implementation of Fully Ceramic Microencapsulated fuel (FCM) in an integral pressurized water reactor (iPWR) with SMR characteristics has been studied previously. FCM has excellent thermal and irradiation resistance properties and is composed of a SiC matrix with dispersed TRISO fuel particles. To perform the thermo-hydraulic analysis of the core of an SMR using FCM as fuel, a computational model was built using CFD codes. The model describes a typical fuel assembly of the reactor and the main thermo-hydraulic parameters are calculated for the increased power values of 65, 80, and 100 MWt. To improve the thermo-hydraulic behavior of the core, it was considered to vary the values of mass flow, core inlet temperature, and system pressure.

Los reactores modulares pequeños (SMR) constituyen una opción innovadora para la generación de energía. Este tipo de reactores ofrece numerosos beneficios y usos. La implementación del combustible microencapsulado cerámico (FCM) en un reactor de agua a presión integral (iPWR) ha sido estudiada con anterioridad. El FCM tiene propiedades térmicas y de resistencia a la irradiación excelentes, y está compuesto por una matriz de SiC donde están dispersas las partículas TRISO. Para realizar el análisis termo-hidráulico del núcleo del reactor propuesto, se construyó un modelo computacional usando un enfoque de Dinámica de Fluidos Computacional (CFD). El modelo construido describe un conjunto combustible típico del reactor y en él se calculan los principales parámetros termo-hidráulicos para diferentes valores de potencia. Para valorar una mejora en el comportamiento termo-hidráulico del núcleo, se consideró variar los valores de flujo másico, temperatura de entrada del refrigerante al núcleo y la presión del sistema.

PACS: Nuclear physics (física nuclear), 29.85.Ca; electroproduction (nuclear reactions) (electroproducción (reacciones nucleares)), 25.30.Rw; cooling and heat recovery of nuclear reactors (enfriamiento y recuperación de calo ren reactors nucleares), 28.41.Fr.

I. INTRODUCTION

Small Modular Reactors (SMRs) are a classification of nuclear reactors according to their electrical power generation capacity (up to 300 MWe); they include different technologies. The interest in the study and development of SMRs in recent years has increased significantly as a consequence of the new challenges of the current energy, technological and economic paradigm. SMRs make it possible to expand the use of nuclear energy to a wider range of customers and energy applications. Their size makes it possible to use nuclear energy in countries that, due to their economic characteristics, are not able to invest in large nuclear power plants. They maintain the advantages of conventional nuclear power plants, such as low greenhouse gas emissions, safety and reliability in energy production, and are heirs to extensive operating experience. Among their advantageous characteristics are the need for lower initial capital investment, their scalability and flexibility in the choice of sites, particularly in remote areas where it is not useful to build traditional nuclear reactors. One of the objectives of the neutronic design of the SMR core is to achieve extended fuel cycles, with the aim of reducing the handling of both fresh and spent fuel to gain proliferation resistance. Due to the small size and modular nature of SMRs, it is possible, when they are part of the same nuclear power plant, to independently manage the modules for maintenance and refueling, while the other modules remain in service. In addition, construction time is reduced because almost all components can be built in factories and installed on-site. All these features allow for shorter licensing times. SMRs have a variety of applications, including cogeneration, hydrogen production, desalination and energy production.

Light water type SMRs (LWRs) have advantages for early deployment, considering that they are the most widely used nuclear technology. Among them, the iPWR integral pressurized water reactors stand out as very promising.

The performance of different types of fuels in SMR designs has been studied for each of these applications. Fully ceramic microencapsulated fuel (FCM), which belongs to the Accident Tolerant Fuel (ATF) group, is one of the most important candidates for use in future LWRs. FCM has excellent thermal performance and irradiation resistance properties. The FCM structure includes the fuel pellets, fuel cladding and gap between the fuel pellets and the cladding. The fuel pellet is composed of a matrix and a large amount of TRistructural-ISOtopic (TRISO) fuel particles that are randomly dispersed in the SiC matrix. The performance of this fuel permits retaining fission products at high burnup rates while maintaining its integrity at temperatures above

1600 °C [1,2].

Previous work has analysed the characteristics of an iPWR reactor using TRISO fuel. In [3], a neutronic analysis was performed for an extended effective two-year fuel cycle at the rated power of a small PWR with TRISO fuel. In [4], a multifactorial study of the influence of variables such as TRISO particle core diameter, packing fraction and enrichment on the fuel cycle length was performed. Also, the thermo-hydraulic analysis with CFD codes of the most loaded fuel assembly was performed considering the axial and radial peak power factors obtained in the study. The study was performed for nominal flow value and stationary cases with loss of coolant. In each case, the average coolant temperature at the outlet of the channel was lower than the saturation temperature. The maximum temperature values in the different materials that make up the fuel were well below the melting limit temperatures.

Based on the previous results in [5], an update of the conceptual design of the reactor core was carried out to reach higher power values. The power density is kept constant and the radial and axial dimensions of the core are increased. The power output was increased to 65 MWt, increasing from 89 fuel assemblies to 157 (FA) and from 150 cm height to 220 cm, and a reduction in fuel cycle length by 1250 effective full power days (EFPD) was obtained. In [6], the neutronic computational model used for the conceptual design was modified to consider two and three burnup zones. The new core design must be completed with a thermo-hydraulic analysis of the proposed power values.

The complex structure of the FCM pellet provides safety advantages for the nuclear power plant [7] but complicates its heat transfer analysis. Heat transfer in FCM pellet is a multi-scale phenomenon that is costly and difficult to model in detail. For simplicity, TRISO fuel particles can be equivalent to homogeneous particles, or even the fuel pellet together with TRISO particles can be equivalent to homogeneous material [1].

In [1], three heat transfer models were built for an FCM pellet: a detailed model for all the layers that make up the fuel (ML). This model homogenizes the TRISO particles (MN) and finally a homogeneous model for the whole pellet. Using the ML model's results as a benchmark, the performance of the MN model of [8] and the homogeneous Maxwell, Chiew-Gland, Beruggeman and EMT models for predicting the maximum and average temperature were discussed.

It was found that the MN model and homogeneous models greatly underestimate the temperature of TRISO fuel particles. The main reason is that these conventional equivalent thermal conductivity (ETC) models do not consider the internal heat source and are not suitable for TRISO fuel particles. Consequently, two new expressions were generated for the equivalent thermal conductivity of TRISO particles that consider the internal heat generation. These expressions start from the equivalence of the average temperature and the maximum temperature between the TRISO particle and the homogeneous equivalent particle. These new improved ETCs better predict the maximum and average temperature of the FCM in both the MN model and the homogeneous model for different values of linear power and packing fraction.

In this work, a computational model of a fuel assembly of the proposed reactor was built using CFD. The model considers the fuel as a homogeneous material, it uses the CFD code Ansys CFX v20.R1 and it incorporates the models described in [1] too. It was calculated for the proposed power values of 65, 80 and 100 MWt, the average temperature values at the outlet of the coolant channel and the maximum temperature values in the fuel and the cladding. To improve the thermo-hydraulic behavior of the core, it was considered to vary the values of mass flow, core inlet temperature and system pressure. Finally, the temperature distributions of the coolant at the outlet of the channel and in the fuel rods in the hottest plane were obtained.

II. MATERIALS AND METHODS

The redesigned reactor core consists of 157 fuel assemblies, the distribution of which is shown in Fig. 1. Each fuel assembly consists of a 5x5 arrangement of fuel rods. The location in the core of the fuel assemblies using control rods and their interior distribution is shown.

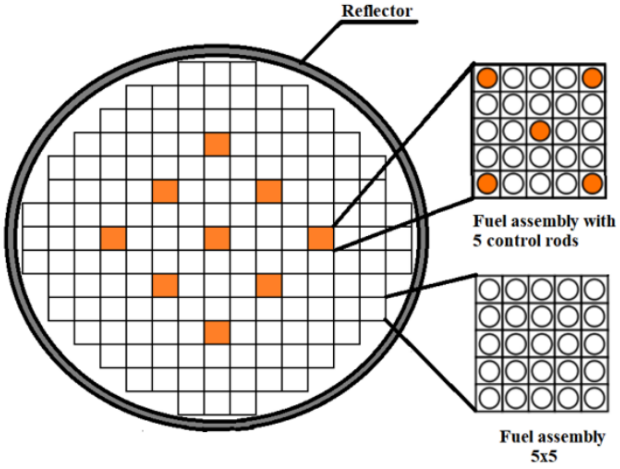

Figure 1. Scheme of the reactor core.

Table 1. Reference core design parameters.

Parameter5	Value / Unit
Power	65 MWt, 80 MWt, 100 MWt
Core height	220 cm
Fuel pitch	3 cm
Fuel rod diameter	2 cm
Clad thickness (Zircaloy)	0.15 cm
Lattice	5x5
Number of control rods	45
Packing fraction	30 %
Enrichment	15 %

The model built for the thermo-hydraulic analysis was developed in ANSYS CFX v20.R1, considering the specified dimensions and describing a typical reactor core fuel

assembly. For the study, the increased reactor power values obtained in previous works are considered [5, 6], which implies higher power density values of the fuel assemblies. The calculations are performed for the fuel assembly with an average reactor power density value and the fuel assembly with the maximum energy release, considering the non-uniformity coefficient of energy release.

Ansys CFX Software v20.R1 is a CFD code focused on the analysis of engineering problems. CFD codes solve the Navier-Stokes equations through numerical methods implemented in the computational domain. The analysis is performed in three fundamental stages: pre-processing, processing and post-processing. The preprocessing stage allows building the geometry of the problem for the discretization of the domain and defining the physical models, material properties and boundary conditions. The processing solves the proposed equations in the discretized control volume, considering the convergence criteria and the defined models. The results obtained can be visualized in the post-processing module.

To simplify our computational model and optimize the available computational resources, the geometry was simplified, taking advantage of the symmetrical configuration of the fuel element. This allows us to take 1/8 of the complete set.

The mesh construction is one of the most important steps in the preprocessing stage. In order to solve for the physical parameters within the constructed geometry, it is necessary to divide the domain into a finite number of small elements. The shape of the mesh and the number of elements used to discretize the domain depend on the geometry and the required accuracy. The method used to generate the mesh was the Multizone method with hexahedron and prismatic elements. This method is based on the meshing of independent zones, providing an automatic decomposition of the geometry into planar regions and free regions. In addition, local configuration tools were used to precise the inflation and size of the elements [9].

In order to eliminate possible numerical effects caused by the mesh size and its distributions, a mesh independency study was performed. The methodology used consisted of generating an initial mesh that was refined once the results converged. First, its size is reduced in the radial direction and then in the axial direction. The results of the meshes are compared, and if the numerical variations between them are less than 2 %, the results are considered independent of the mesh size. The variable chosen to perform the analysis is the temperature in the coolant.

To check the quality of the mesh, an evaluation is carried out considering the Orthogonal Quality and Skewness indicators. According to these statistics, it can be affirmed that the mesh obtained meets the requirements established for both indicators since an average value for Orthogonal Quality of 0.99028 and a maximum value for Skewness of 0.52497 were obtained [9].

The resulting mesh has a total of 174870 nodes and 151140 elements. In the radial direction, the maximum size of the elements has a value of 2 mm in the fuel rods and a value of 1 mm in the coolant. In the axial direction the maximum size of the elements is 50 mm. In the refrigerant-cladding interface the mesh is refined using the inflation option: Total Thickness.

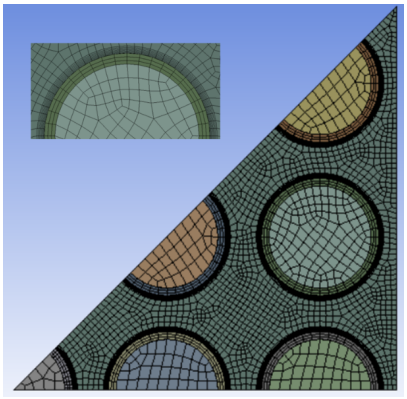

Figure 2. Generated mesh.

TRISO fuel particles are composed of a core, a porous carbon buffer layer (buffer), an inner pyrolytic carbon (IPyC) layer, a silicon carbide (SiC) layer and an outer pyrolytic carbon (OPyC) layer [4]. Fig. 9 represents the structure of FCM pellets and TRISO fuel particles.

The encapsulating material, together with the TRISO particles, was considered as a homogeneous material. The EMT model, equations (1, 2, 3), will be used in conjunction with the improved ETC for the TRISO particles [1], which led to equation (4) to calculate the equivalent thermal conductivity of the homogeneous material. The equivalent specific heat for the fuel pin was calculated as a mass-weighted average of the values of C_p values of each material comprising the pin [10].

$$k_e = [k \cdot A + \sqrt{k^2 \cdot A^2 + \frac{k}{2}}]k_c \tag{1}$$

$$A = \frac{3F - 1 + \frac{2-3F}{k}}{4} \tag{2}$$

$$k = \frac{k_d}{k_c} \tag{3}$$

$$\frac{1}{ETC_{maxT}} = \frac{1}{k_1}\frac{r_5}{r_1} + \sum_{i=2}^{5} \frac{2r_5}{k_i}(\frac{1}{r_{i-1}} - \frac{1}{r_i}) \tag{4}$$

Where k_e is the conductivity of the homogeneous material, $k_c$is the thermal conductivity of the matrix, and k_d is the ETC of the TRISO fuel particle, F is the packing fraction of the TRISO particle in the fuel rod, k_i and r_i is the thermal conductivity

and radius, respectively of each layer of the particular TRISO, Fig. 3.

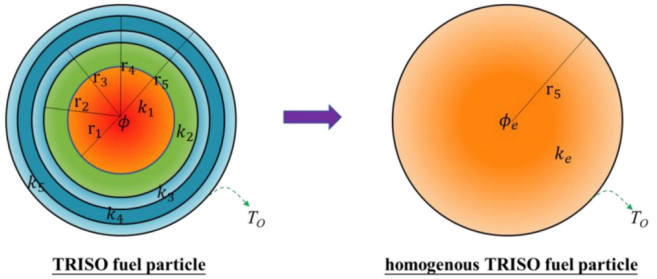

Figure 3. The diagram of the equivalent relationship from TRISO fuel particle to homogenous one.

Table 2 shows the values of density, the source of thermal conductivity and specific heat and the values of radius of the fuel rod, the gap and the cladding. The values of the radius of the layers that make the TRISO particles are also shown. The constant values were taken from [4].

Table 2. Dimension and properties of the TRISO particle.

Material layer	Density g/cm^3	Thermal conductivity (W/m·K)	Specific heat (J/kg·K)	Radius (cm)
UO2 Kernel	10.88	(eq. 5)	(eq. 6)	0.03
Buffer layer	1.1	1.0	710	0.04
IPyC layer	1.9	4.0	710	0.045
SiC layer	3.2	(eq. 7)	(eq. 8)	0.0458
OPyC layer	1.9	4.0	710	0.0535
SiC matrix	3.2	(equ. 7)	(eq. 8)	1.0
He gap	0.179	0.1415	5240	1.0085
Fuel cladding	6655	(eq. 9)	(eq. 10, 11)	1.1585

$$k_{UO_2} = \frac{100}{7.5408 + 17.692\tau + 3.6142\tau^2} + \frac{6400}{\tau^{5/2}} e^{-\frac{16.35}{\tau}} \quad (5)$$

$$C_{P_{UO_2}} = 52.17 + 87.95 - 84.24\tau^2 + 31.54\tau^3 - 2.63\tau^4 + 0.71\tau^{-2} \quad (6)$$

$$k_{SiC} = (-0.003 + 1.05 \cdot 10^{-5} T)^{-1} \quad (7)$$

$$C_{P_{SiC}} = 925.65 + 0.3772T - 7.9259 \cdot 10^{-5} T^2 - \frac{3.1946 \cdot 10^7}{T^2} \quad (8)$$

$$k_{Zir} = 14 + 0.0115T \, , 300 \leq T \leq 1100K \quad (9)$$

$$C_{pZir} = 221 + 0.172T - 5.87 \cdot 10^{-5} T^2 \, , 300 \leq T \leq 1100K \quad (10)$$

$$C_{pZir} = 380 \, , 1100 \leq T \leq 1600K \quad (11)$$

$$\tau = T/1000 \quad (12)$$

Equations (5), (6), (9), (10), (11), (12) were taken from [11] for UO_2 and Zirconium-niobium (2.5 %) alloy type N–2.5 (E-125) and equations (7) and (8) for SiC from [12].

The distributions as a function of temperature for the specific heat and thermal conductivity obtained for the homogeneous material are shown in Fig. 3 and 4, which were fitted to a polynomial of degree 3 for C_p and of degree 6 for k_e.

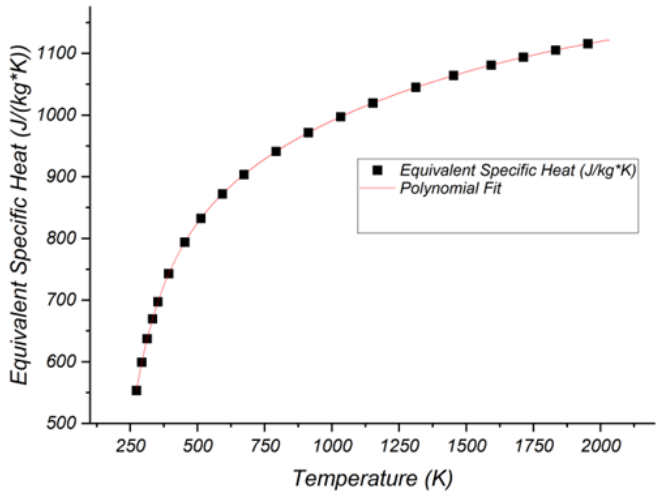

Figure 4. Polynomial fitting C_p.

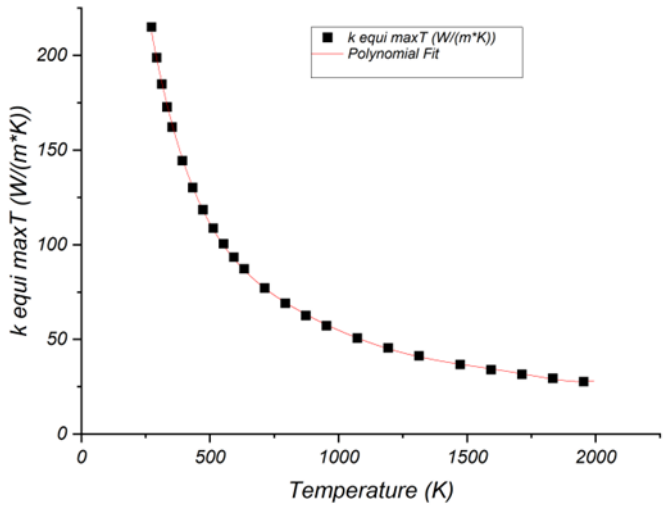

Figure 5. Polynomial fitting k_e.

In the CFD model, three domains were established in the fuel elements: fuel, cladding and coolant. The materials that define them, their main properties, the boundary conditions and the turbulence and heat transfer models were defined. The k-e standard turbulence model was selected due to the simplicity of the physical and geometrical model to be studied, which provides accurate results with a low computational cost. The temperature-dependent properties of water were

obtained from the IAPWS-IF97 library included in the material libraries provided by ANSYS, according to the International Association for Properties of Water. This is a formulation of water and its properties for industrial uses, designed for fast and complex calculations. The Steam5l material is selected for water, with parameters varying for temperatures between 450 and 900 K and pressures between 1000 and 30000 kPa. The heat transfer in the gap was considered through the Thin Material model [9]. The axial distribution of the normalized power density calculated in a previous works was used [6].

III. RESULTS AND DISCUSSION

Different values of mass flow, core inlet temperature and system pressure were studied to describe the thermo-hydraulic behavior of the proposed reactor core. The study was carried out for different values of increased power with the objective of demonstrating that the reactor core from the thermohydraulic point of view is safe in each case. To guarantee this safety, the temperature at the coolant channel outlet has to be lower than the saturation temperature with a reserve of approximately 30 K, similar to conventional reactors [13]. In addition, the maximum temperatures in the fuel and the cladding must be lower than the melting limit temperatures of the materials composed.

The methodology used consisted of first considering a constant power density distribution by height. The mass flow that guarantees a temperature increase throughout the channel was determined, ΔT, of approximately 20 K. This criterion is based on the fact that conventional reactors have ΔT of approximately 40 K and much higher heights (AP1000: 4.2 m and 3400 MWt). We start from a coolant mass flow for the whole core of 393, 591 and 924 kg/s for 65, 80 and 100 MWt, respectively. These values are divided by the number of fuel assemblies and by 8 to obtain the flow through 1/8 of the fuel assembly equally. The system pressure is equal to 6 MPa, and the temperature at the channel inlet T_i = 461 K , similar to that used in [4]. For a power of 65 MWt, the power density of the core with these dimensions is the same as the core described in [4] with 25 MWt, and for the values of 80 MWt and 100 MWt, the power density increases. Table 3 shows the results obtained, where $\dot{m}$ is the mass flow rate, $T_o$is the average coolant temperature at the outlet of the channel and T_{max} the maximum temperature.

Table 3. Results for mass flow variation.

Power (MWt)	$\dot{m}$ (kg/s)	ΔT (K)	T_o (K)	T_{max} Clad (K)	T_{max} UO_2 (K)
65	393	37.9	499.4	546	624
65	591	25.7	487.1	531	607
65	739	20.9	482.3	524	600
65	924	17	478.3	518	593
80	591	31.3	492.7	545	640
80	739	25.4	487	538	631
80	924	20.7	482	530	623
100	924	25.6	487	546	663
100	1155	20.8	482.2	537	651

The mass flow values selected were 739, 924 and 1155 kg/s for 65, 80 and 100 MWt, which are the values that guarantee a ΔT of approximately 20 K. From the mass flow values obtained, new calculations were performed taking into account the axial distribution of thermal power density of the fuel elements. It is increased T_i for different values of system pressure. The value of 6 MPa of the base design can be increased if we consider values up to 15 MPa of conventional PWR nuclear reactors. In addition, the simulation is performed for the most loaded fuel assembly by taking the radial peaking factor (PF) reported in each case for the start of the fuel cycle [6]. The temperature T_i was increased considering the saturation temperature for the different pressure values, 549 K, 568 K and 584 K. The T_o was limited to maintain an average reserve of approximately 30 K of the saturation temperature as a safety criterion against an accident with loss of coolant.

As shown in tables 4, 5 and 6, each case complies with the thermo-hydraulic safety parameters described above. The maximum temperatures obtained in the fuel and the cladding are well below the allowable limit of safe operation in all cases.

It has been estimated that gaseous fission products begin to be released at a limit temperature of 1873.0 K [14, 15], and the maximum allowable temperature in the cladding is 1477.2 K [16].

Table 4. Calculated for 65 MWt of power.

T_i (K)	P (MPa)	FP	ΔT (K)	T_o (K)	T_{max} Clad (K)	T_{max} UO_2 (K)
473	6	1	19.8	493	551	677
473	6	1.95	37.6	510.8	617.5	875
503	8	1	19	522	579	706
503	8	1.95	35.7	538.8	643	902
523	10	1	18.3	541.5	598	725
523	10	1.95	34.2	557.4	660	920

Table 5. Calculated for 80 MWt of power.

T_i (K)	P (MPa)	FP	ΔT (K)	T_o (K)	T_{max} Clad (K)	T_{max} UO_2 (K)
473	6	1	19.9	493	560	718
473	6	1.9	36.4	509.5	632	945
503	8	1	19.1	522.3	588	747
503	8	1.9	34.8	538	658	973
523	10	1	18.1	541.3	607	766
523	10	1.9	33.3	556.5	675	991

Table 6. Calculated for 100 MWt of power.

T_i (K)	P (MPa)	FP	ΔT (K)	T_o (K)	T_{max} Clad (K)	T_{max} UO_2 (K)
473	6	1	20	493.2	570	767
473	6	1.92	36.3	509.5	654	1050
503	8	1	19.2	522.3	598	796
503	8	1.92	34.6	537.8	679	1078
523	10	1	18.4	541.6	616	815
523	10	1.92	33.2	556.4	695	1097

Table 7 shows the summary results for a pressure value of 10 MPa and t_i = 523 K for the different power values.

Table 7. Summary of parameters for increased power values.

Power (MWt)	ṁ (kg/s)	FP	ΔT (K)	T_o (K)	T_{max} Clad (K)	T_{max} UO_2 (K)
65	739	1	18.3	541.5	598	725
65	739	1.95	34.2	557.4	660	920
80	924	1	18.1	541.3	607	766
80	924	1.9	33.3	556.5	675	991
100	1155	1	18.4	541.6	616	815
100	1155	1.92	33.2	556.4	695	1097

In addition, for the case of more extreme thermo-hydraulic conditions (last case in table 7), the coolant temperature distribution at the channel outlet (Fig. 6), the temperature distribution in the fuel in the central plane (Fig. 7) and the radial temperature distribution for the hottest pin (Fig. 8) were calculated.

Figure 5 shows how the maximum temperature value at the outlet of the channel in the coolant, 580 K, is reached at points near the fuel rods. These values are lower than the saturation temperature value at the considered working pressure of 10 MPa.

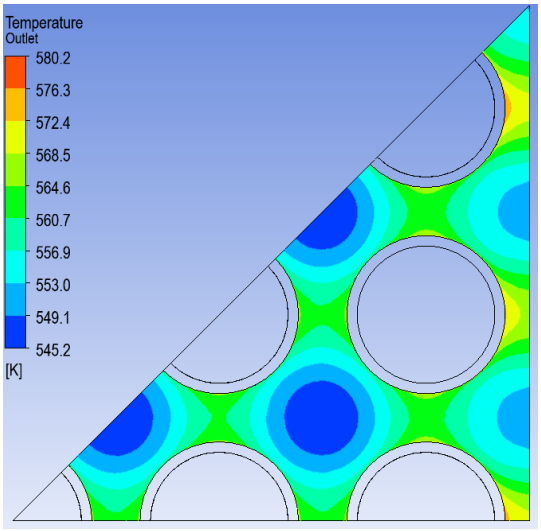

Figure 6. Coolant outlet temperature profile.

Figure 7 shows the radial distribution of fuel rod temperature values in the plane where the maximum temperature value is reached. The average temperature value of each fuel rod is approximately 1060 K. The fuel rod that reaches the highest temperature value is in the upper right corner. This value is 1097 K, which is below the 1800 K reported as the limit value for a reactor with this type of fuel. As the fuel rods were considered to be a homogeneous material, this maximum temperature value represents the average value of the maximum temperatures of the TRISO particles. Therefore, there are higher temperature values in some TRISO particles, specifically in the UO_2 layer. However, due to the characteristics of this type of fuel and the values obtained, there is a very large reserve.

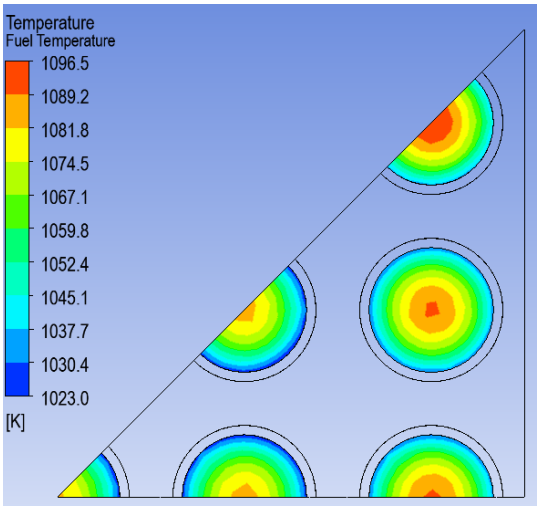

Figure 7. Fuel temperature profile in the central XY plane on the axial direction.

Figure 8 shows the temperature profile inside the hottest fuel pin. As can be observed, it is quite flattened because it is considered a homogeneous mixture of its constituent materials.

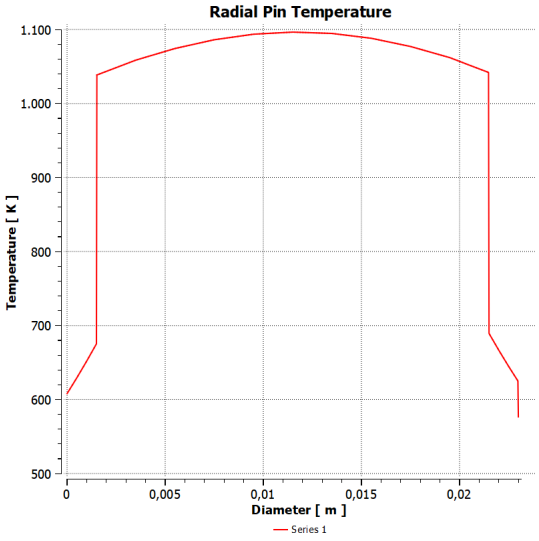

Figure 8. Radial temperature distribution in the central pin.

IV. CONCLUSIONS

In this work, a computational model was built based on the CFD codes of ANSYS CFX v20.R1 of a typical Small Modular Reactor fuel assembly. This is an Integral Pressurized Water Reactor using FCM as fuel. The model considers the fuel pellets as a homogeneous mixture and accurately describes the thermo-hydraulic parameters of the fuel assembly.

With values of increased powers of 65, 80, and 100 MWt, mass flow values that guarantee a temperature increase in the channel of 20 K for a typical fuel assembly with average power density are obtained. In addition, the values of coolant

temperature at the channel outlet are obtained, which allows an average reserve of 30 K of the saturation temperature for the most loaded fuel assembly at working pressures of 6, 8, and 10 MPa. In all the calculated cases, the maximum temperature values in the cladding and fuel are far from the limits allowed for this type of reactor. In order to obtain a higher efficiency of the thermo-hydraulic cycle, it is recommended to increase the coolant temperature values at the channel inlet and working pressure.

REFERENCES

[1] M. Wang, S. Bu, B. Zhou, Z. Li, and D. Chen, Nucl. Eng. Technol. **55**, 1140 (2023).

[2] D. Schappel, K. Terrani, J. Powers, L. Snead, and B. Wirth, Nucl. Eng. Des. **335**, 116 (2018).

[3] A. Hussain and C. Xinrong, Prog. Nucl. Energy **52**, 531 (2010).

[4] J. Rosales, J.-L. François, A. Ortiz, and C. García, Nucl. Eng. Des. **387**, 111599 (2022).

[5] C. García, J. Rosales, J. L. François, R. Granados, and H. Martínez, Rev. Cub. Fis. **39**, 76 (2022).

[6] R. Granados, C. García, J. Rosales, and D. Domínguez, in XXVI ENMC Brasil, (2023).

[7] Q. Deng, S. Li, D. Wang, Z. Liu, F. Xie, J. Zhao, J. Liang, and Y. Jiang, Nucl. Eng. Technol. **54**, 3095 (2022).

[8] Q. Libo, Y. Hongxing, S. Yufa, D. Jian, C. Wei, L. Yu, D. Sijia, and S. Danhong, Nucl. Power Eng. **41**, 69 (2020).

[9] Ansys, ANSYS CFX Solver Theory Guide ANSYS, Inc. Southpointe 2600 ANSYS Drive Canonsburg, PA 15317, 2020).

[10] L. García Fajardo, Çonceptual design of a system controlled by an accelerator for waste transmutation nuclear and energy applications". PhD Thesis, Universitat Politècnica de València, Valencia, 2012.

[11] V. Bobkov, L. Fokin, E. Petrov, V. Popov, V. Rumiantsev, and A. Savvatimsky, "Thermophysical properties of materials for nuclear engineering: a tutorial and collection of data", (International Atomic Energy Agency, Vienna, 2008).

[12] L. L. Snead, T. Nozawa, Y. Katoh, T.-S. Byun, S. Kondo, and D. A. Petti, J. Nucl. Mater **371**, 329 (2007).

[13] Westinghouse,. AP1000 Design Control Document Rev. 19. Section 4.3. (2011) https://www.nrc.gov/docs/ML1117/ML11171A445.pdf.

[14] K. Fukuda, S. Kashimura, T. Tobita, and T. Kikuchi, Nucl. Eng. Des. **157**, 221 (1995).

[15] O. Ö. Gülol, Ü. Çolak, and B. Yıldırım, J. Nucl. Mater. **374**, 168 (2008).

[16] Code of Federal Regulations, FR **72**, 49508 (2007).

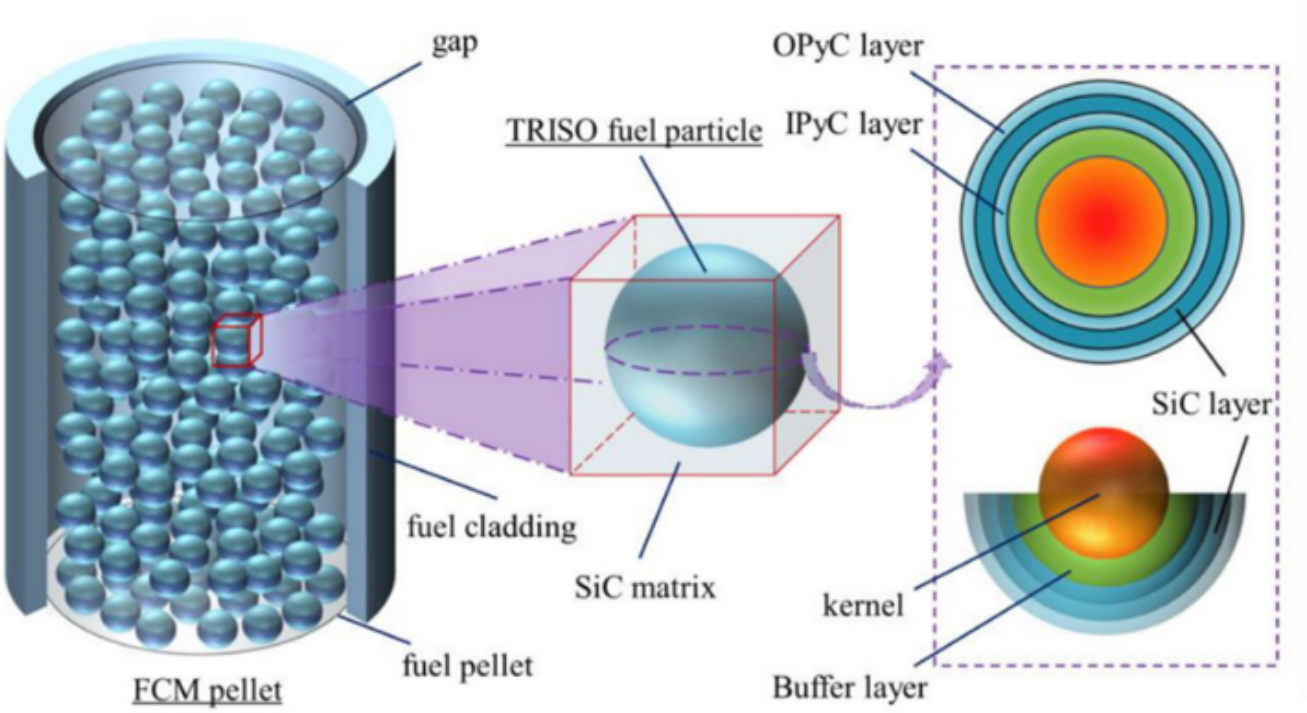

Figure 9. FCM pellet and TRISO fuel particle structure.